J|A|C|S ARTICLES

Published on Web 08/12/2010

Mechanism of Substrate Shuttling by the Acyl-Carrier Protein within the Fatty Acid Mega-Synthase

Claudio Anselmi,[†] Martin Grininger,[‡] Preeti Gipson,[§] and José D. Faraldo-Gómez*[,†,||]

Theoretical Molecular Biophysics Group and Department of Structural Biology, Max Planck Institute of Biophysics, Frankfurt am Main, Germany, Department of Membrane Biochemistry, Max Planck Institute of Biochemistry, Martinsried, Germany, and Cluster of Excellence 'Macromolecular Complexes', Frankfurt am Main, Germany

Received April 20, 2010; E-mail: jose.faraldo@biophys.mpg.de

Abstract: Fatty acid mega-synthases (FAS) are large complexes that integrate into a common protein scaffold all the enzymes required for the elongation of aliphatic chains. In fungi, FAS features two independent dome-shaped structures, each 3-fold symmetric, that serve as reaction chambers. Inside each chamber, three acyl-carrier proteins (ACP) are found double-tethered to the FAS scaffold by unstructured linkers; these are believed to shuttle the substrate among catalytic sites by a mechanism that is yet unknown. We present a computer-simulation study of the mechanism of ACP substrate-shuttling within the FAS reaction chamber, and a systematic assessment of the influence of several structural and energetic factors thereon. Contrary to earlier proposals, the ACP dynamics appear not to be hindered by the length or elasticity of the native linkers, nor to be confined in well-defined trajectories. Instead, each ACP domain may reach all catalytic sites within the reaction chamber, in a manner that is essentially stochastic. Nevertheless, the mechanism of ACP shuttling is clearly modulated by volume-exclusion effects due to molecular crowding and by electrostatic steering toward the chamber walls. Indeed, the probability of ACP encounters with equivalent catalytic sites was found to be asymmetric. We show how this intriguing asymmetry is an entropic phenomenon that arises from the steric hindrance posed by the ACP linkers when extended across the chamber. Altogether, these features provide a physically realistic rationale for the emergence of substrate-shuttling compartmentalization and for the apparent functional advantage of the spatial distribution of the catalytic centers.

Introduction

Fatty acids constitute an important energy source for many organisms and are essential components of all biological membranes. They are also important in extra- and intracellular signaling, as their derivatives include hormones and second messengers. Synthesis of fatty acids entails the iterative elongation of an aliphatic chain through a series of chemical reactions, which are essentially conserved across all life forms: first, acetyltransferase (AT) and malonyl/palmitoyl transferase (MPT) load acetyl primer and malonyl substrates from coenzyme A (CoA) to a phosphopantetheine (PPT) prosthetic group covalently bound to an acyl-carrier protein (ACP). Next, the ketoacyl synthase (KS) condenses the substrate to acetoacetyl-ACP in a decarboxylative reaction. The three subsequent reaction steps, catalyzed by ketoacyl reductase (KR), dehydratase (DH), and enoyl reductase (ER), lead to the fully saturated acyl-ACP, which can serve directly as a primer for the next condensation reaction. In each reaction cycle the growing acyl-chain is elongated by two carbons, until the complete fatty acid is transferred back to CoA by MPT.[1−8]

In most bacteria and plants, these enzymes are spatially independent (type II), and the synthesis reaction relies on the abundance of ACP, which exists as a soluble protein transporting the chemical intermediates.[9,10] Remarkably, however, other higher organisms have evolved large multifunctional synthases (type I) that integrate all the necessary components. In fungi, for example, fatty acid synthase (FAS) is a large 2.6-MDa heterododecameric complex made up by a central wheel of six α subunits and two domes of three β subunits each, arranged 3-fold symmetrically (Figure 1).[2−8] The two domes thus enclose two independent reaction chambers, each of which is lined by three copies of all the enzymes required for the iterative fatty

[†] Theoretical Molecular Biophysics Group, Max Planck Institute of Biophysics.
[‡] Department of Membrane Biochemistry, Max Planck Institute of Biochemistry.
[§] Department of Structural Biology, Max Planck Institute of Biophysics.
[||] Cluster of Excellence 'Macromolecular Complexes'.

(1) Lynen, F. *Eur. J. Biochem.* **1980**, *112*, 431–442.
(2) Lomakin, I. B.; Xiong, Y.; Steitz, T. A. *Cell* **2007**, *129*, 319–332.
(3) Jenni, S.; Leibundgut, M.; Maier, T.; Ban, N. *Science* **2006**, *311*, 1263–1267.
(4) Jenni, S.; Leibundgut, M.; Boehringer, D.; Frick, C.; Mikolasek, B.; Ban, N. *Science* **2007**, *316*, 254–261.
(5) Leibundgut, M.; Jenni, S.; Frick, C.; Ban, N. *Science* **2007**, *316*, 288–290.
(6) Leibundgut, M.; Maier, T.; Jenni, S.; Ban, N. *Curr. Opin. Struct. Biol.* **2008**, *18*, 714–725.
(7) Johansson, P.; Wiltschi, B.; Kumari, P.; Kessler, B.; Vonrhein, C.; Vonck, J.; Oesterhelt, D.; Grininger, M. *Proc. Natl. Acad. Sci. U.S.A* **2008**, *105*, 12803–12808.
(8) Gipson, P.; Mills, D. J.; Wouts, R.; Grininger, M.; Vonck, J.; Kuhlbrandt, W. *Proc. Natl. Acad. Sci. U.S.A* **2010**, *107*, 9164–9169.
(9) Campbell, J. W.; Cronan, J. E., Jr. *Annu. Rev. Microbiol.* **2001**, *55*, 305–332.
(10) White, S. W.; Zheng, J.; Zhang, Y. M.; Rock, C. O. *Annu. Rev. Biochem.* **2005**, *74*, 791–831.

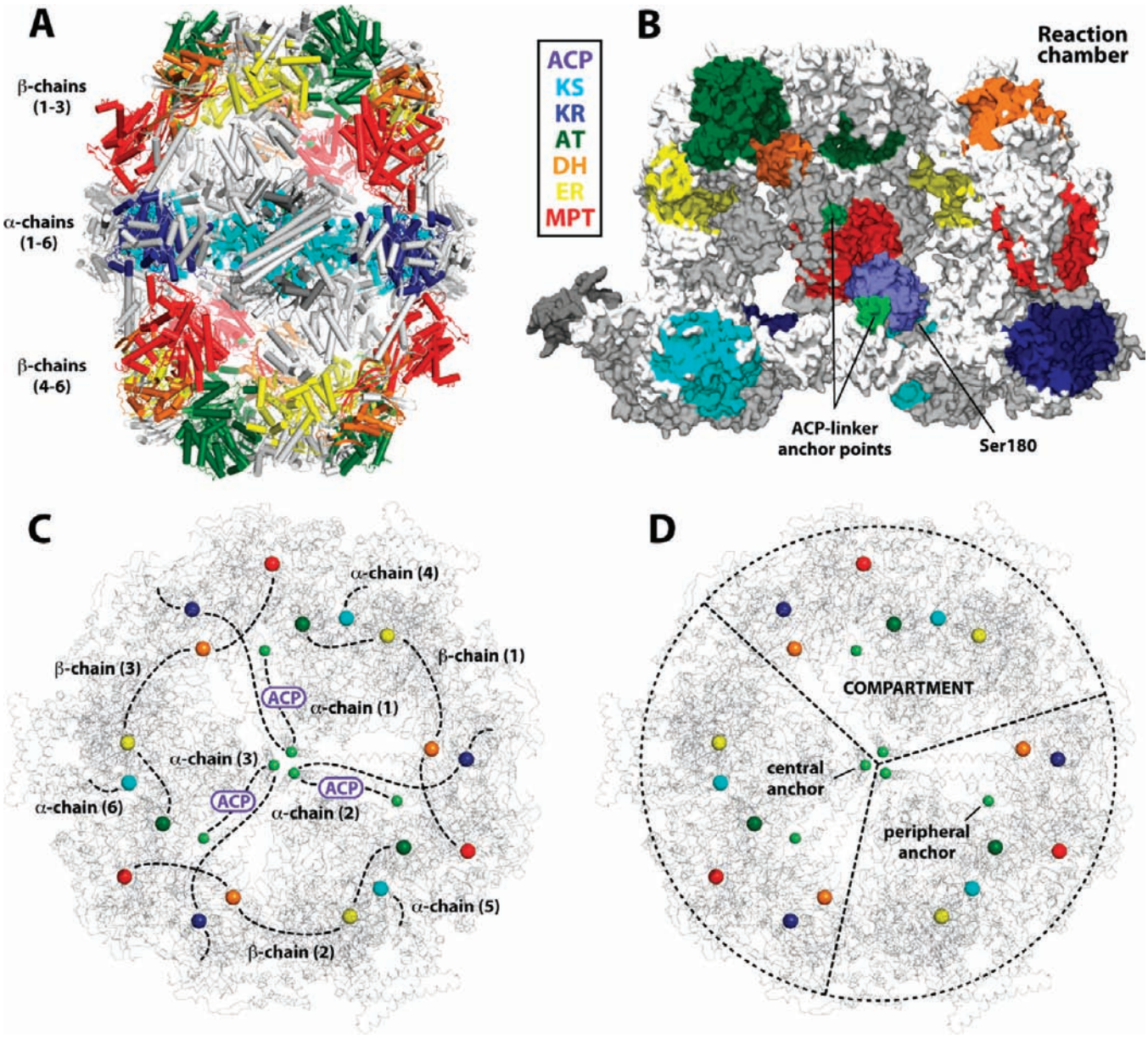

Figure 1. Structure of the fungal fatty acid synthase. (A) Side-view cartoon representation of the double-domed FAS reaction chamber. The catalytic domains are colored following the scheme in the legend; three ACP domains are found inside each dome, double-tethered to the β-chain scaffold and to the central α-chain wheel by two unstructured linkers. (B) Close-up view of the interior of the reaction chamber, showing one ACP domain stalled at KS; the location of Ser180 and of the two linker anchor points on the chamber wall are indicated. (C, D) View of a reaction chamber from above. The catalytic sites and ACP−linker anchor points are indicated with colored spheres. In panel C, the polypeptide connectivity between catalytic domains, ACP, and anchor points is schematically indicated with dashed lines. In panel D, dashed lines indicate how these can be divided in three independent sets, according to their location relative to the peripheral-linker anchor points; each of these sets thus defines a catalytic compartment.[2−4]

acid elongation. In addition, each chamber includes three ACP, double-tethered by flexible linkers; one of these is anchored at the wall of the chamber scaffold (peripheral linker) and the other at the center of the α-wheel (central linker).[2−6,8] This solution ensures a high effective concentration of ACP inside the reaction chamber, presumably further catalyzing the synthesis reaction.[1,3,7]

The mechanism of ACP shuttling within the FAS chamber is, however, essentially unknown. Crystal structures of FAS have consistently shown the ACP bound to the KS site at the chamber equator,[5,7] and although partial occupancy of other catalytic sites has been detected in a recent cryoelectron microscopy study,[8] fundamental questions remain open. For example, are the ACP domains confined inside their corresponding reaction subcompartments or can they reach all three catalytic-site copies in each chamber? Is their motion stochastic, or do they follow preferred pathways as they deliver the substrate from site to site, as has been proposed elsewhere?[5,7] And what is the functional advantage, if any, of the ACP double-tethering to the FAS scaffold, and of the intriguing spatial arrangement of the catalytic sites? Can the three ACP domains in each chamber be seen as independent from one another, or are they somehow coupled? And last, what is the extent to which the dynamics of the ACP domains is influenced by the flexible linkers or by long- or short-range interactions with the chamber wall and the catalytic sites? In this paper we present a systematic, multiscale simulation study of the dynamics of the ACP domains inside a FAS reaction

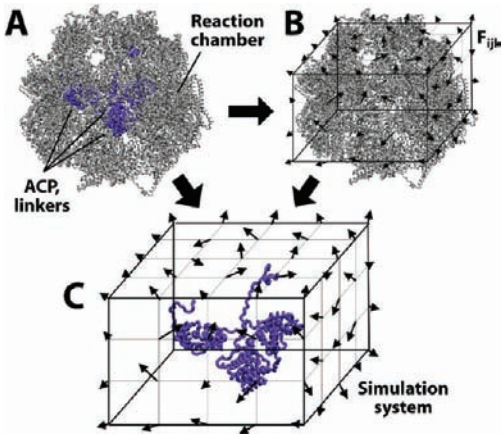

Figure 2. Schematic diagram of the simulation protocol. The simulations pertain to one of the chambers and the three ACP domains therein. This initial construct (A) is partitioned into a mobile and a static portion. The mobile portion consists of three ACP domains plus the corresponding linkers, anchored at their ends. The static portion consists of all other domains comprising the reaction chamber. Forces arising from interactions of a probe particle with the chamber were computed and mapped a priori on a cubic grid (B). During the subsequent simulations of the motion of the ACP/linker triplet, these external forces are extrapolated to the actual atomic positions (C) and added to the forces originating within the mobile portion. Notwithstanding the simplicity of the model, the combined computer time of these simulations exceeds 250 000 h, as we have aimed to achieve optimal sampling under all simulation conditions.

chamber, which has enabled us to gain nontrivial and unexpected insights into these questions.

Methods

Simulation Details. The simulation system comprises one FAS reaction chamber; that is, six α-chains at the equatorial wheel, three β-chains constituting a dome, and three double-tethered ACP domains. Two structures were initially considered, one obtained with X-ray crystallography (PDB entry 2VKZ),[7] and another through a reconstruction based on cryo-EM, single-particle microscopy data (EM database accession number EMD-1623).[8] In both cases the ACP linkers and other missing loops facing the chamber interior were modeled, using Modeler 9v3.[11] Neither the α-subunit segment from residue 541 to 598 nor the C-terminal domains from residue 1748 were included in the model, because both segments reside outside the reaction chamber. The data shown in Figure 3A were obtained with both X-ray and EM structures, giving comparable results; therefore, only the EM reconstruction was employed in all subsequent calculations.

A multiscale approach was adopted to study the shuttling of the ACP domains among the catalytic sites (Figure 2). Specifically, the model comprises a coarse-grained (CG), semirigid-body representation of the ACP domains, a CG, flexible representation of the ACP−scaffold linkers, a lattice-based representation of the FAS chamber, and an implicit description of solvent (constant friction and dielectric constant); cofactors within KR and ER sites were not included (see legend of Figure 3). The elastic potential used for the ACP domains pertains to the Cα trace and consists of pairwise, harmonic distance restraints within a 1-nm range. The lattice model of FAS consists of two regular cubic grids of 231 × 233 × 185 points, isotropically spaced by 0.1 nm, onto which we mapped the electrostatic and van der Waals forces originating from the scaffold. These are computed using a probe particle placed at each grid point in the lattice and stored for subsequent use. During the simulations, the actual forces acting on the ACP domains and linkers are derived from those mapped on the lattice at each time step, by trilinear interpolation and scaling according to the specific nonbonded parameters of the explicit CG atoms, e.g., charge. In summary, we simulate the dynamics of three interacting ACP domains and their respective linkers (1341 CG particles), fixed at their end points, under the influence of a constant force field originating from the FAS reaction chamber. This multiscale approach is noticeably less computationally demanding than one in which all interaction sites in the system are simulated explicitly. We estimate the speed-up of the calculation to be 50-fold, compared to a standard simulation using cutoff and neighbor-list algorithms, and about 10-fold, if the nonbonded interactions within the FAS scaffold are excluded from the calculation, i.e., fixing the corresponding CG particles. This lattice-based simulation algorithm is implemented in a modified version of GROMACS 4.0.3.[12]

The equations of motion (Langevin) were integrated with a time step of 10 ps; the collision frequency was 0.2 ps^{-1}. All bond lengths were kept fixed with the LINCS algorithm.[13] All simulations were performed with modified version of the MARTINI CG force field:[14,15] as in the standard MARTINI implementation, nonbonded interactions were described by a shifted Lennard−Jones potential cutoff at 1.2 nm; however, the attractive part of the potential was scaled down to prevent aggregation, in the absence of explicit-water interactions. In keeping with the parametrization of the MARTINI CG forcefield, a uniform dielectric constant $\varepsilon = 15$ mimics electrostatics screening.

Lastly, ACP sampling distributions were derived using VolMap in VMD 1.8.6.[16] Residence times at each catalytic center were evaluated from the integral of the ACP density distributions within 3.0 nm from each center; this definition results in no spatial overlap among sites and thus no ambiguity in the statistics.

Linker Elasticity and Persistence Length. To model the dynamics of the ACP−scaffold linkers, we considered two alternative models of different elastic properties and analyzed each in terms of their persistence length. The persistence length, *P*, is a means to quantify the stiffness of a long polymer. The *P* value approximately defines the length threshold beyond which the dynamics of a polymer is no longer accurately represented by a flexible elastic rod, but rather by a three-dimensional random walk. The expected *P* values for unstructured polypeptide chains are distributed around 1 nm,[17,18] that is, a value much smaller than any conceivable characteristic length of the ACP linkers (25 and 45 amino acids). Thus, the concept of 'elastic spring' is not applicable to long polypeptides such as these linkers; a beads-on-a-string, stochastic model is much more appropriate. The *P* values of the linker models used in this study were evaluated through simulations of both peripheral and central linkers alone and analysis of the corresponding end-to-end distance distributions (Figure 4B). For the first model (P_{upper}), these distributions are almost Gaussian around average values of 5.3 and 3.6 nm for the peripheral and central linker, respectively. In the context of the worm-like chain model,[19] these profiles are consistent with persistence lengths *P* equal to 0.9 and 0.7 nm, respectively. The second model (P_{lower}) differs from the first one in that Cα atoms at positions *i* and $i + 4$ along the chain are biased to be closer together; the resulting persistence length is $P \sim 0.5$ nm for both linkers. Taken together, the two models approximately correspond to the upper and lower limits

(11) Šali, A.; Blundell, T. L. *J. Mol. Biol.* **1993**, *234*, 779–815.
(12) Berendsen, H. J. C.; van der Spoel, D.; van Drunen, R. *Comput. Phys. Commun.* **1995**, *91*, 43–56.
(13) Hess, B.; Bekker, H.; Berendsen, H. J. C.; Fraaije, J. G. E. M. *J. Comput. Chem.* **1997**, *18*, 1463–1472.
(14) Marrink, S. J.; Risselada, H. J.; Yefimov, S.; Tieleman, D. P.; de Vries, A. H. *J. Phys. Chem. B* **2007**, *111*, 7812–7824.
(15) Monticelli, L.; Kandasamy, S. K.; Periole, X.; Larson, R. G.; Tieleman, D. P.; Marrink, S. J. *J. Chem. Theory Comput.* **2008**, *4*, 819–834.
(16) Humphrey, W.; Dalke, A.; Schulten, K. *J. Mol. Graph.* **1996**, *14*, 33–38.
(17) Sarkar, A.; Caamano, S.; Fernandez, J. M. *J. Biol. Chem.* **2005**, *280*, 6261–6264.
(18) Li, H.; Oberhauser, A. F.; Redick, S. D.; Carrion-Vazquez, M.; Erickson, H. P.; Fernandez, J. M. *Proc. Natl. Acad. Sci. U.S.A* **2001**, *98*, 10682–10686.
(19) Kratky, O.; Porod, G. *Rev. Trav. Chim. Pays-Bas* **1949**, *68*, 1106–1123.

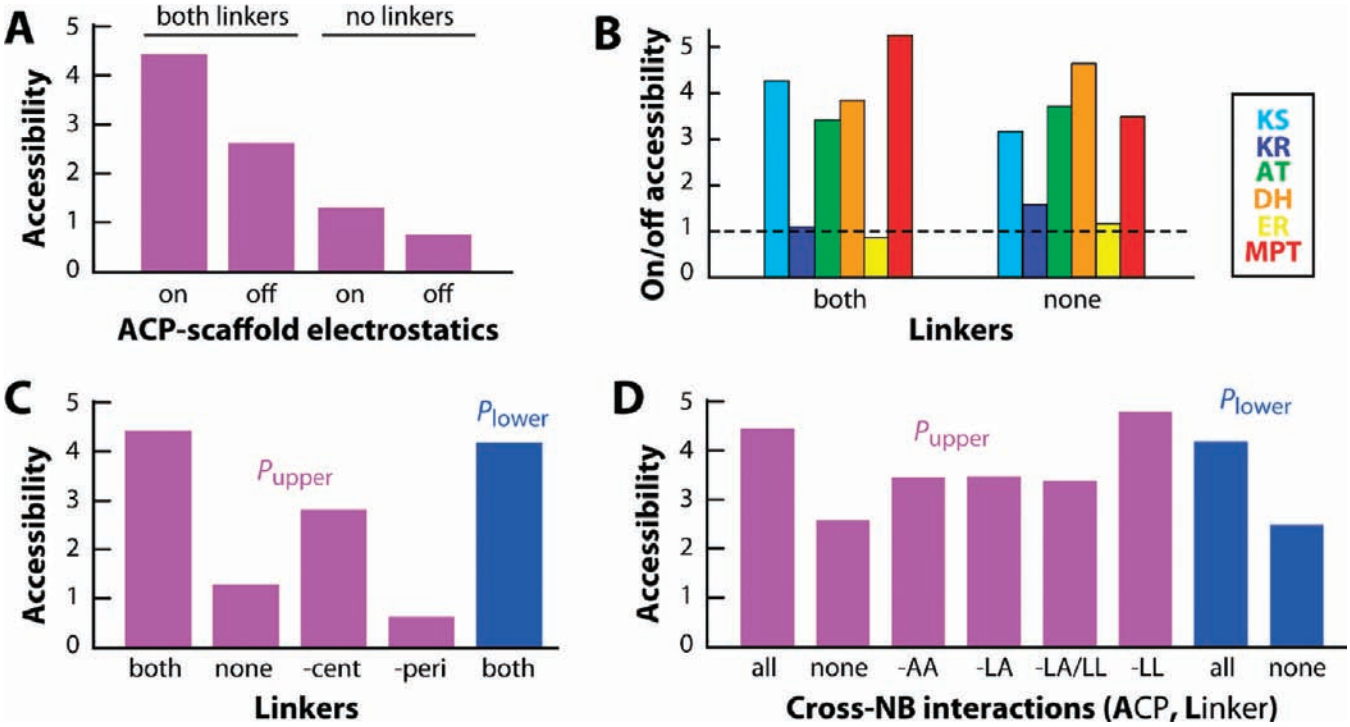

Figure 3. Probability of ACP encounters with catalytic centers, or accessibility. All values are normalized with respect to a reference simulation where all ACP−scaffold linkers were deleted and in which ACP−ACP cross-NB interactions were also excluded. (A) Influence of electrostatic interactions between ACP and the FAS scaffold, in simulations with and without ACP linkers. (B) Influence of electrostatic interactions between ACP and the scaffold on the accessibility to each specific set of catalytic centers. The values plotted are ratios of the accessibility with electrostatics 'on', over that with electrostatic interactions 'off'. As shown, electrostatics enhance the accessibility to KS, AT, DH, and MPT, while that to ER and KR is only slightly affected, whether in the presence of *both* or *none* of the linkers. Equivalent results were obtained when cofactors were included within the ER and KR sites (data not shown). (C) Influence of the linkers on the overall accessibility. Values are shown from the simulations with *both* and *none* of the linkers (same as in panel A), as well as with just the peripheral (-cent) or the central (-peri) linkers. Magenta and blue colors refer to the two persistence-length (P) values used to model the elasticity of the linkers (see Figure 4B). (D) Influence on site accessibility of specific contributions to the nonbonded interactions between sets of ACP/linkers. Data are shown from simulations including *all* or *none* of these contributions, as well as from those excluding ACP−ACP (-AA), linker−ACP (-LA), and/or linker−linker (-LL) interactions.

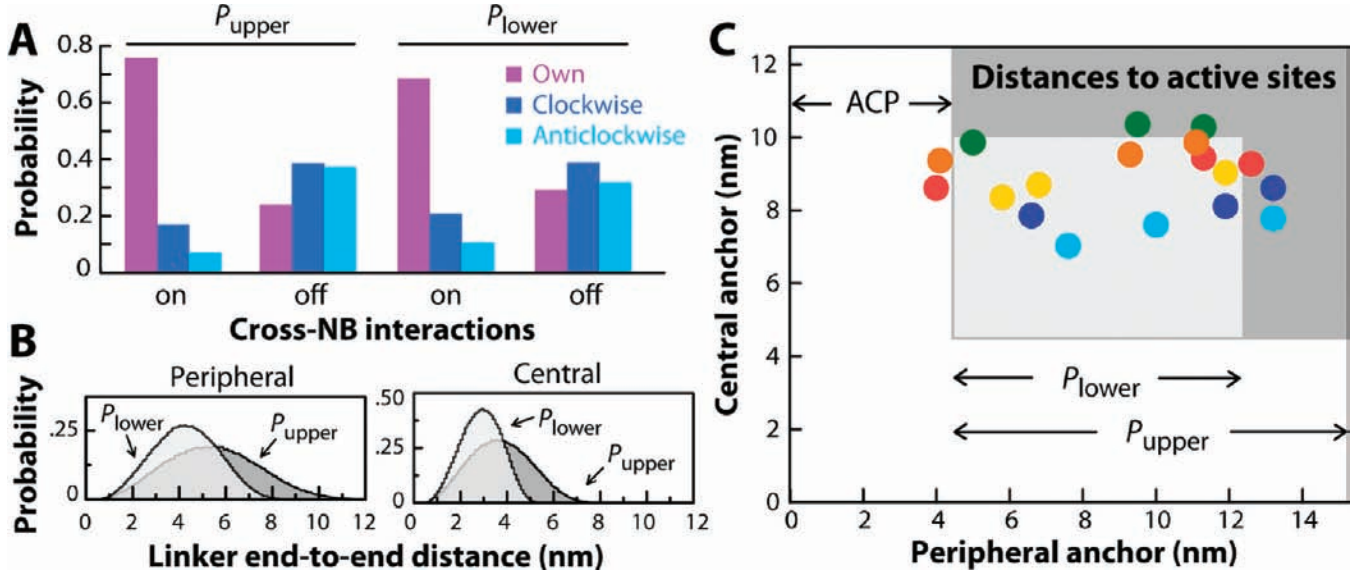

Figure 4. Influence of linker elasticity on ACP dynamics. (A) Probability of ACP-site encounters in different catalytic compartments depending on whether cross-NB interactions are included (on) or excluded (off) and on the persistence-length (P) model used; ACP can reside in its own compartment or move to those adjacent in the clockwise or anticlockwise directions (viewed from the top). (B) End-to-end distance distributions for the peripheral (45 residues) and central linkers (25 residues), when simulated individually, for the two parametrizations considered in this study (see Methods). The resulting persistence-length values, P_{upper} and P_{lower}, are 0.9 and 0.5 nm for the peripheral linker, and 0.7 and 0.5 nm for the central linker. (C) Distances between active sites and the central- and peripheral-linker anchor points within each compartment. The color scheme is the same as in Figure 1. All distances are offset on account of the ACP dimensions (from linker end-points to Ser180). The gray boxes indicate the range of distances accessible to the ACP domains, for each of the linker P values considered in this study. Note that the linker lengths in a β-sheet conformation would exceed this range significantly (17.1 and 9.5 nm for peripheral and central linkers, respectively).

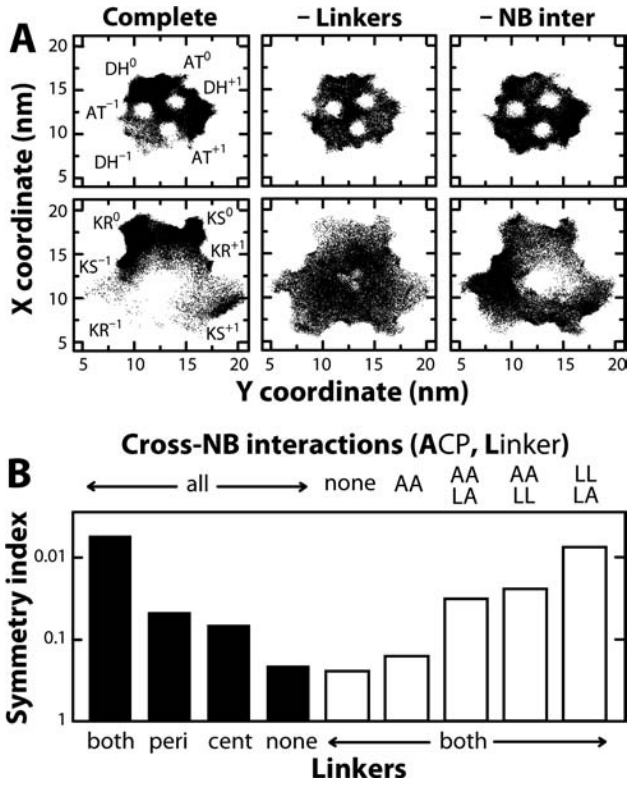

Figure 5. Emergence of ACP compartmentalization and sampling asymmetry. (A) Projection of the space sampled by the ACP domains (represented by the trajectory of Ser180) in proximity to the tip of the dome (top panel: AT, DH sites) and at the level of the FAS equator (lower panel: KS, KR sites). The coordinate system adopted is such that *z* is parallel to the reaction-chamber axis and $x-y$ parallel to the equatorial plane. The approximate positions of the catalytic sites are indicated. Sites labeled with '0' correspond to the ACP domains' own compartment; those adjacent in the clockwise direction (viewed from the top) are labeled with a '+', while those anticlockwise are labeled with a '−'. The sampling data derived from the three ACP domains in the chamber are overlaid, through a ± 120° rotation around the chamber axis so as to superimpose the '0' sites of each domain. ACP sampling distributions are shown for simulations of the full-length system including all NB interactions (complete), when the ACP−scaffold linkers are deleted (-linkers) or when the cross-NB interactions are neglected (-NB inter). (B) Influence of linkers and cross-NB interactions on the symmetry of the ACP sampling distributions (see Methods). Notations are the same as for Figure 3.

of the range of most probable *P* values expected for an average polypeptide chain.[17,18]

Quantification of Compartmentalization and Symmetry. The symmetry index used in Figure 5B is defined as $1 - \langle e^2 \rangle = (b^2 + c^2)/2a^2$, where *a*, *b*, and *c* correspond to the residence probability of a given ACP in each compartment. No compartmentalization occurs if $a = b = c$, and therefore $1 - \langle e^2 \rangle = 1$; by contrast, when compartmentalization is perfect, $b = c = 0$ and then $1 - \langle e^2 \rangle = 0$. However, some residual asymmetry is always expected due to finite sampling. Therefore, $1 - \langle e^2 \rangle$ is never exactly equal to 0 or 1. In addition, for a given simulation condition, the asymmetry of the ACP sampling differs among the six catalytic centers (Figure 5A). For clarity we have therefore defined the symmetry-index as the log-average of $1 - \langle e^2 \rangle$ over the different catalytic sites.

Results

Computational Approach and Trajectory Analysis. By construction, computer models used in molecular-dynamics simulations must include a set of mathematical functions that describe all interatomic interactions contributing to motion within the system, some empirical and some derived directly from physical laws. It is therefore an advantage of simulation studies to be able to selectively modulate or even exclude some of these contributions so as to discern the determinant factors of a given dynamic process. The philosophy of this approach is not unlike that underlying directed mutagenesis, domain truncation, gene knockout, etc. To gain insights into the mechanism of ACP shuttling within FAS, we have adopted such a strategy systematically, using a coarse-grained molecular model (See Figure 2 and Methods). Thus, we have analyzed the ACP dynamics with or without the linkers tethering them to the chamber wall, or selectively removing just the peripheral or central linker, or after varying their characteristic persistence length. To determine the influence of long-range steering forces on the ACPs, we have compared simulations where the energy function included or excluded electrostatic interactions between the ACP and the FAS scaffold. To assess the importance of volume-exclusion effects, a series of simulations were also carried out in which all nonbonded (NB) interactions between different ACPs and their linkers were selectively suppressed, effectively allowing them to overlap in space. In total, 18 simulation conditions were considered. For each, 40 μs of simulation time was computed, split into 200 independent trajectories of the ACP triplet; 7.6 million configurations were thus collected for each simulation condition.

All analysis of the ACP trajectories hereafter is in actuality focused on Ser180 (Figure 1), as this is the residue to which the growing acyl chains are bound, through the PPT prosthetic group, while the ACP shuttles among the enzymatic sites. In addition, because the FAS reaction chamber is 3-fold symmetric and all ACPs are equivalent, unless noted otherwise the statistics presented here combine the sampling obtained for each of them, after the appropriate rotation around the chamber axis.

Contributing Factors for ACP Steering toward Catalytic Centers. On the basis of the available structural data, it has been suggested that electrostatic interactions may play an important role during ACP shuttling in FAS.[2,8,20−24] Our results are consistent with this notion of electrostatic steering; in simulations where the electrostatic interactions between the ACPs and the FAS scaffold were excluded, the probability of finding an ACP at a catalytic center was indeed ∼45% lower; a similarly marked decrease (35%) upon removal of electrostatic interactions was also observed when the ACPs were detached from their anchor points, i.e., when the linkers were deleted (Figure 3A). Nevertheless, electrostatic forces should not be thought of as a dominant factor of the ACP dynamics, as in such a case they would hinder efficient substrate shuttling, especially for sites with strong electrostatic complementarity, e.g., KS or MPT (Figure 3B). This is illustrated by simulations in which we doubled-up the magnitude of the electrostatic forces, which makes the ACP stall at this catalytic site.

From our simulations it also clear that the ACP−scaffold linkers are extremely important for steering the ACP domains toward the catalytic centers, in that they promote the orientation

(20) Parris, K. D.; Lin, L.; Tam, A.; Mathew, R.; Hixon, J.; Stahl, M.; Fritz, C. C.; Seehra, J.; Somers, W. S. *Structure*. **2000**, *8*, 883–895.
(21) Zhang, Y. M.; Rao, M. S.; Heath, R. J.; Price, A. C.; Olson, A. J.; Rock, C. O.; White, S. W. *J. Biol. Chem.* **2001**, *276*, 8231–8238.
(22) Zhang, Y. M.; Wu, B.; Zheng, J.; Rock, C. O. *J. Biol. Chem.* **2003**, *278*, 52935–52943.
(23) Zhang, Y. M.; Marrakchi, H.; White, S. W.; Rock, C. O. *J. Lipid Res.* **2003**, *44*, 1–10.
(24) Rafi, S.; Novichenok, P.; Kolappan, S.; Zhang, X.; Stratton, C. F.; Rawat, R.; Kisker, C.; Simmerling, C.; Tonge, P. J. *J. Biol. Chem.* **2006**, *281*, 39285–39293.

in which Ser180 faces the active sites. Deletion of the linkers drops the probability of successful encounters between ACP/Ser180 and the catalytic sites by ~70% (Figure 3C). The directing effect of the peripheral linker seems to be more pronounced than that of the central linker, as deletion of the latter reduces the same probability only by ~35%; when only the central linker is present, but the peripheral one is deleted, the effect is much more pronounced.

Lastly, volume exclusion effects also play a role in modulating ACP shuttling. When all nonbonded (NB) interactions among ACP domains and linkers are excluded, the probability of finding an ACP at a catalytic site drops by ~40% (Figure 3D). ACP−ACP and ACP−linker interactions seem to contribute equally to this effect, as individual exclusion of each of these terms lowers the probability to the same extent (~20%). By contrast, when linker−linker NB interactions are excluded, a small positive effect on the residence probability is observed (<10%); such a variation is, however, probably within the expected statistical uncertainty. These last observations pertaining to volume-exclusion effects suggest that the size of the ACP domain does influence shuttling inside the confined reaction chamber. Smaller ACP domains would be less likely to visit the catalytic sites, and so larger sizes would be, at least to some degree, favored from a mechanistic standpoint. In this regard, it is worth noting that although the structure of the ACP core, containing Ser180 and the PPT prosthetic group, is similar for plant and bacterial homologues, the overall size of the yeast ACP domain is about twice that of the freestanding bacterial ACP.[5,25]

Linker Elasticity, ACP Compartmentalization, and Symmetry. An interesting concept emerging from the original crystallographic studies of FAS is that of compartments or subspaces inside the reaction chamber within which the dynamics of the ACP domains is somewhat confined.[2−4] Each of these compartments would consist of a unique set of enzymatic sites contributed by adjacent β chains, as depicted in Figure 1C,D. The putative confinement of each ACP domain within the corresponding compartments has been attributed to the intrinsic elastic properties of the linkers, which would be tuned to preclude excursions into adjacent compartments.

Our simulations are consistent with the concept of compartment, but they are clearly in disagreement with the notion that the length or intrinsic elasticity of the native linkers hinders the ACP motion within the reaction chamber. This is best illustrated by a simulation in which we uncouple the triplet of ACP/linkers, by suppressing all cross-NB interactions among them. That is, in effect ACP−linkers in different compartments can overlap in space without penalty and move independently. As shown in Figure 4A, under these conditions the ACP domains sample the catalytic sites in the 'adjacent' compartments with equal or greater probability than their 'own'. This is shown for two alternative parametrizations of the linker elastic properties (Figure 4B; see Methods), which are meant to reproduce the most likely persistence-length values for an average, unstructured polypeptide chain.[17,18] For the lower-bound model (parametrized so that $P = 0.5$ nm), the probability of sampling all compartments is roughly equal; for the upper-bound model ($P = 0.7-0.9$ nm), adjacent compartments are actually visited more often, by a factor of ~1.5. This is due to the fact that to accomplish their most likely elongation in the upper-bound model, linkers effectively 'push' the ACP domains away from their 'own' compartment. In conclusion, our analysis provides no indication that the ACP motion is hindered within the reaction chamber by the length or elasticity of the native linkers. This is consistent with a purely geometric analysis of the distances between the catalytic sites and the linkers' anchor points on the FAS scaffold (Figure 4C); if we adjust for the dimensions of the ACP domain (~4.5 nm along the axis from Ser180 to the linker ends) and consider an intermediate persistence-length value within the above-mentioned range, it seems clear that most if not all catalytic sites are in principle accessible to all ACP domains.

Notwithstanding the lack of linker-induced confinement, our results support the concept of compartmentalization of substrate shuttling. As shown in Figure 4A, simulations in which the NB interactions between ACP/linkers are restored show a greater bias in favor of the ACP domains' own compartment (~70%), for both persistence-length models. When the adjacent compartments are compared, the sampling probability of the catalytic sites in the anticlockwise direction is about 2-fold smaller than in the clockwise, when viewed from the dome of the chamber (Figure 4A). As illustrated in Figure 5A, this intriguing asymmetry is most pronounced for the catalytic sites close to the equator, i.e., KS and KR, although to a lesser extent it can also be observed at the chamber top.

Therefore, compartmentalization of the ACP dynamics seems to emerge from volume-exclusion rather than linker-length constraints. To elucidate the specific origin of this asymmetric dynamics, we considered again a series of simulations where one or both linkers were deleted, as well as those where the cross-NB interactions between ACP/linkers sets are progressively excluded. For these, a symmetry index was computed that reflects the degree of similarity in the sampling of catalytic sites in the 'own' and 'adjacent' compartments, in the clockwise and anticlockwise directions (see Methods).

As may be expected, near-perfect 3-fold symmetry in the sampling was obtained if both peripheral and central linkers are absent, or, as mentioned above, if all cross-NB interactions are excluded (as these underlie volume-exclusion effects) (Figure 5AB). Consistent with this, compartment sampling is also highly symmetric when the ACP−ACP interactions are restored but not linker−linker or ACP−linker interactions. By contrast, introduction of linker−linker and ACP−linker interactions, but not ACP−ACP, results in asymmetric sampling, to a degree similar to that of the complete, fully interacting system. Taken together with the observation that asymmetry is most pronounced at the FAS equator, we conclude that compartmentalization arises from the steric hindrance imposed by the linkers of each ACP domain on the motion of the other ACP domains and their linkers, that is, on their ability to explore different catalytic sites.

ACP Trajectories and the Spatial Disposition of the Catalytic Sites. The spatial arrangement of the catalytic centers around the peripheral ACP anchor points, taken together with the assumption that the ACP motion is tightly restrained by the linkers, have also led to the notion that ACP delivers substrates to the enzymatic sites in well-defined trajectories, e.g., following a two-dimensional circular pathway.[2,4] Our simulations, however, give no indication of such preferential 2-D trajectories, as means by which the ACP domain can deliver substrates among catalytic sites with improved efficiency. Rather, ACP-domain motion resembles 3-D stochastic diffusion; consequently, many site-to-site translations occur that would not be chemically productive, i.e., that do not follow the ideal order of the elongation reaction (Figure 6A). This stochasticity notwithstanding, it can be argued that the spatial distribution of the enzymatic sites, approximately positioned along a circular path, does indeed favor substrate delivery, simply because (stochastic,

(25) Roujeinikova, A.; Simon, W. J.; Gilroy, J.; Rice, D. W.; Rafferty, J. B.; Slabas, A. R. *J. Mol. Biol.* **2007**, *365*, 135–145.

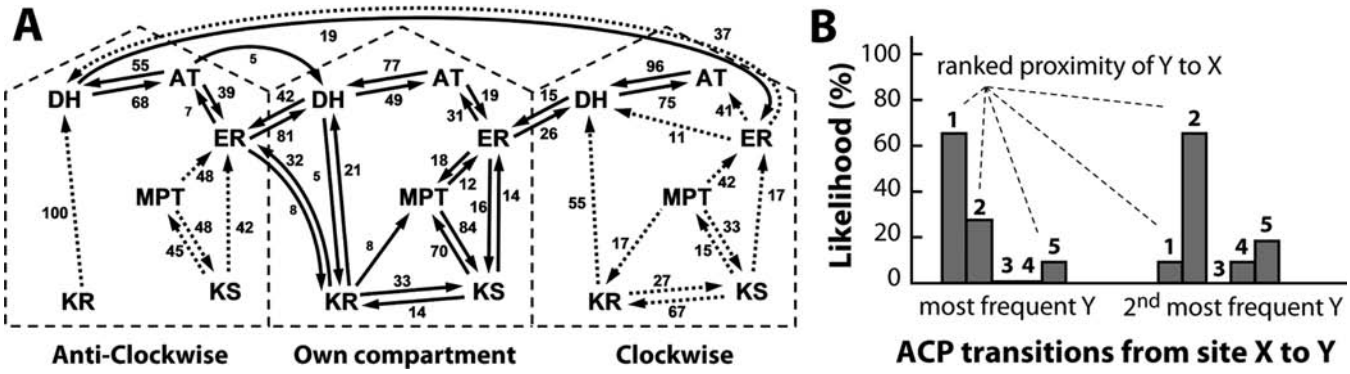

Figure 6. Stochastic nature of ACP shuttling among enzymatic sites. (A) For each site, the most significant transition probabilities (>5%, solid arrows) to all other sites in the FAS reaction chamber are indicated alongside the direction of the transition. Dashed arrows indicate those transitions that are observed with lower frequency during the simulations. The data for all three ACP domains are combined by classifying the site-to-site transitions according to the compartment where they occur, i.e., within the ACP-domain's own compartment, or across/within those adjacent in the clockwise or anticlockwise directions. The acyl-chain elongation reaction proceeds as MPT/AT → $(KS \rightarrow KR \rightarrow DH \rightarrow ER)_7$ → MPT. (B) Correlation between site-to-site shuttling probability and proximity. When an ACP domain moves away from a catalytic center, X, the most frequently visited site thereafter, Y, happens to be the closest, for ∼65% of the cases; for the remainder ∼25%, Y corresponds to the second closest catalytic center. Likewise, the second most frequent transition from X is with the second most proximal site Y in most cases.

three-dimensional) excursions among adjacent sites occur with greater probability than among distant sites (Figure 6B). In fact, we observe that the ACP domains at a given catalytic center shuttle preferentially to the subsequent one in the reaction cycle, directly or after one misstep (Figure 6).

Discussion

FAS and other mega-synthases are essential chemical factories for the cell. Their versatility and modularity also makes them promising subjects in biotechnological and chemical-design applications. Yet, the mechanism of substrate shuttling within these synthases is unknown, largely due to the lack of experimental data that directly probes the dynamical nature of these complex systems. In this study we set out to assess this mechanism and to formulate a plausible hypothesis, using computer-simulation methods. This is a considerable challenge; each FAS reaction chamber is approximately 25 nm^3 and comprises ∼1.4 million protein and solvent atoms. To be able to derive a statistically meaningful analysis of the dynamics of the ACPs inside this chamber, we have therefore adopted a multiscale approach that reduces the complexity of the system. The simplifications thus introduced preclude us from analyzing, for example, the differential specificity of the catalytic sites or the actual chemistry of elongation of the acyl chain. However, the model preserves the physical properties of the system that we consider to be essential for the mechanism of ACP shuttling between catalytic centers.

Of particular importance is the degree of flexibility of the linkers that anchor each ACP to the reaction chamber. Because any CG model will describe the elastic properties of these linkers only approximately, we have cross-validated all our results with two different parametrizations, chosen to yield persistence-length values within known experimental bounds for unstructured polypeptides. Our model does oversimplify features that are undoubtedly crucial for protein−protein recognition or reaction kinetics; however, these features are too short-ranged to influence the process of ACP shuttling across distances of tens of nanometers. While the prominence of such short-range effects may be inferred from the crystalline structures of FAS, in which the ACPs are consistently stalled at the KS sites,[5] more recent cryo-EM data in the unconstrained, solution state, convey a rather different picture. Here, the ACPs are seen to be diffused across the reaction chamber and to transiently associate with different catalytic centers, none of which seems to have a dominant affinity.[8]

A main finding from this study is that a given ACP can visit essentially all catalytic centers in the 3-fold symmetric reaction chamber, unhindered by the length or characteristic flexibility of the linkers that tether it to the chamber scaffold. This finding is at odds with the hypothesis that the ACPs are confined in a circular trajectory within their own reaction-chamber compartment, by virtue of the limited elasticity of these linkers.[2,4] Thus, rather than following well-defined pathways, our simulations reveal that the ACPs trajectories are essentially stochastic, albeit coupled to one another, primarily through a volume-exclusion effect.

That is not to say, however, that the linkers have no influence on the ACP dynamics. Indeed, an unexpected and intriguing result from this study is that when a given ACP moves across compartments, its linkers, now extended across the chamber, constitute a steric hindrance for the other ACPs and their linkers. That is, their ability to sample a range of catalytic sites is diminished. The result of this complex multibody interaction is a net asymmetry in the sampling of the catalytic centers; that is, although by symmetry all three ACPs move identically, the preferred configurations are those in which the ACP domains reside in their own compartment or, to a lesser degree, in the one adjacent in the clockwise direction (viewed from the top). Thus, compartmentalization does occur, but it emerges as an entropic effect due to 'molecular crowding' rather than because of linker-length constraints.

Likewise, the stochasticity of the ACP motions does not imply that the positioning of the catalytic sites, roughly in a circular path that mimics the acyl-chain elongation reaction, has no relevance. Rather, we have shown that the spatial proximity of sites that are consecutive in the catalytic cycle results in a greater number of excursions between them, versus more distant sites. However, it should be noted that many site-to-site excursions also occur that would be functionally unproductive.

Interestingly, a similar self-organization strategy may be used by modular polyketide synthases (PKS). This is another class of multifunctional enzymes, presumably evolved from FAS, which are able to produce an extremely varied ensemble of compounds by combinatorial biosynthesis methods.[26,27] The chemical variability of the products arises from the substrate specificity of the catalytic domains, modulated by the proba-

(26) Shen, B. *Curr. Opin. Chem. Biol* **2003**, *7*, 285–295.
(27) Walsh, C. T. *Acc. Chem. Res.* **2008**, *41*, 4–10.

bilistic occurrence of reactions during chain growth. Therefore, it is plausible that the spatial reorganization of the different PKS modules influences the synthesis reaction, as we propose for FAS, by introducing a probability bias on the range of substrate-shuttling trajectories. More specific studies would of course be necessary to validate this hypothesis.

Lastly, we note that previous experimental and computational studies of the bacterial single-enzyme FAS components[2,8,20−24] have proposed that ACP recognition is facilitated by the electrostatic complementarity of the respective protein surfaces;[2,23] indeed, the structure of yeast FAS with the ACP domains docked at different sites confirmed that electrostatics contacts can form between ACP and the scaffold.[8] Our simulations clearly concur with this notion, as evidenced by the observation that suppressing the electrostatic interactions between the chamber and the ACP domains drastically reduces the residence time of the latter in the vicinity of most of the catalytic sites.

Conclusions

We have presented a physical model of the dynamics of ACP domains within the 3-fold symmetric FAS reaction chamber. Although the approximations adopted preclude a detailed analysis of the association between ACP domains and the catalytic sites, the model captures the physical properties relevant to the mechanism of ACP shuttling among them. In summary, this study suggests that the mechanism of ACP-mediated shuttling may be seen as essentially stochastic, restricted only by 'molecular crowding' effects arising from the cross interactions between the ACP domains and their linkers and modulated by electrostatic steering forces. We have thus provided a physically realistic explanation to the emergence of ACP compartmentalization within reaction subchambers and to the seeming functional advantage afforded by the spatial disposition of the catalytic sites. By contrast, this study contradicts the notion that the elastic strain on the ACP−scaffold linkers has a determining influence on ACP dynamics, particularly so as to impose precisely defined trajectories through space.

Acknowledgment. We thank Janet Vonck and Werner Kühlbrandt for their valuable insights into the structure of FAS and for making available their unpublished cryo-EM structure, and to Dieter Oesterhelt and Filipp Oesterhelt, for helpful discussions early on in the project. We are also thankful to Lucy Forrest and Janet Vonck for their detailed revision of this manuscript. This work was partially funded by the DFG Cluster of Excellence 'Macromolecular Complexes'. Computer time was provided in part by the Leibniz-Rechenzentrum.

JA103354W